JOC The Journal of Organic Chemistry

Article

pubs.acs.org/joc

Selective Binding Affinity between Quaternary Ammonium Cations and Water-Soluble Calix[4]resorcinarene

Meiling Hong, Ying-Ming Zhang, and Yu Liu*

Department of Chemistry, State Key Laboratory of Elemento-Organic Chemistry, Collaborative Innovation Center of Chemical Science and Engineering (Tianjin), Nankai University, Tianjin 300071, P. R. China

Supporting Information

ABSTRACT: An amphiphilic calix[4]resorcinarene bearing four hydrophilic sulfonate sites at the upper rim and four hydrophobic *n*-pentyl chains at the lower rim (SR4A5) was synthesized by sulfonation of tetramethoxyresorcinarene. The molecular binding behaviors of SR4A5 with different types of organic cations, i.e., singly and doubly charged aliphatic ammonium salts and singly and doubly charged π-aromatic ammonium salts, were comprehensively investigated by means of ^{1}H NMR, fluorescence, and UV/vis spectroscopic titration experiments. The competitive binding titrations demonstrate that, superior to the reported *p*-sulfonatocalix[4]arene systems, the stability constants upon association with SR4A5 can reach up to 10^6 M^{-1} order of magnitude in water, ultimately leading to better binding affinity and molecular selectivity toward dicationic guests. Significantly, UV/vis spectroscopic experiments further revealed that the specific binding behaviors of SR4A5 with bispyridinium guests can be attributed to the charge transfer interaction between electron-rich and electron-deficient aromatics upon host−guest complexation. These obtained results provide an effective strategy to realize the highly selective molecular recognition process with multiply charged macrocyclic receptors and will definitely promote the development of the field of water-soluble resorcinarene-based supramolecular assemblies.

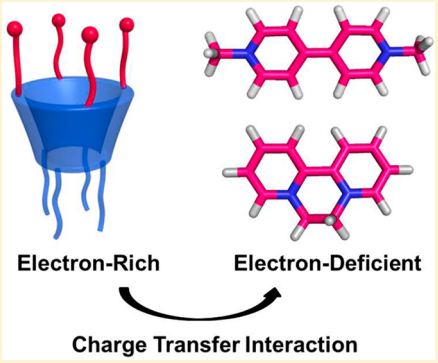

INTRODUCTION

Calixarenes, defined as a class of "cyclic oligonuclear phenolic compounds" in a broad sense, have shown great potential as multifunctional synthetic receptors in miscellaneous fields. In terms of molecular structure and reaction conditions, the term "calixarene" in a narrow sense especially specifies the ones obtained from the reaction of formaldehyde with *p*-alkylphenols under basic conditions, whereas the resorcinol-derived calixarenes, called resorcinarenes, can be synthesized by acid-catalyzed condensation with various aromatic and nonaromatic aldehydes.[1] To date, as representative water-soluble calixarene derivatives, the sulfonated ones that contain phenolic units linked by methylene groups at the *ortho* positions and modified by sulfonate sites at the *para* position (SC*n*As, *n* = 4−8) have been widely utilized in fluorescent sensing,[2] crystal engineering,[3] virus inhibition,[4] enzyme assays,[5] drug release,[6] and pesticide detoxification,[7] mainly through the synergistic effect with the sulfonate sites at the upper rim and the hydroxyl groups at the lower rim as well as the intrinsic hydrophobic cavity enclosed by phenolic rings. However, in contrast to these known SC*n*A systems, the research on sulfonated calixarenes and resorcinarenes is unevenly developed, and there is a relative paucity of studies on the molecular binding behaviors of water-soluble resorcinarene tetramers.[8] Consequently, it is imperative to systematically investigate the molecular recognition systems involving water-soluble resorcinarenes, on the basis of which supramolecular cooperativity can be stimulated to facilitate the formation of more advanced nanoassemblies in water.

Motivated by our ongoing interest in the host−guest recognition and thermodynamic analysis of *p*-sulfonatocalix[4]arene (SC4A) and its analogues,[7,9] we herein report the selective molecular binding behaviors between an amphiphilic calix[4]resorcinarene (SR4A5) and a series of quaternary ammonium cations, with the aim to comprehensively demonstrate the molecular binding characteristics of water-soluble resorcinarenes. As a good supplement to the existing well-known SC4A-based systems, it has been revealed that apart from the regular electrostatic attraction with sulfonates, the charge transfer interaction is one of the important driving forces in controlling the unique binding behaviors with SR4A5. The structural features of the host SR4A5 in this work can gather some inherent advantages together. First, the cavity of SR4A5, which resembles the one of SC4A, is intrinsically a three-dimensional and π-electron-rich scaffold to selectively encapsulate guest molecules. Second, the flexible alkyl chains on either side of the cyclic tetramers can not only access the role of amphiphilicity to enhance aggregation stability[10] but also elongate the vertical depth of the cavity, by which the resorcinarene backbone could be endowed with adaptive capacity to some specific substrates.[11] Third, the multiple

Received: December 14, 2014
Published: January 13, 2015

DOI: 10.1021/jo502825z
J. Org. Chem. 2015, 80, 1849−1855

sulfonate groups, which are the source of power for water solubility, can also offer primary electrostatic binding sites especially for organic cations, while in association with these sulfonate groups, the $-OCH_3$ moieties as electron-donating groups at the upper rim can further enhance the electronegativity throughout the whole cavity of the resorcinarene. Therefore, we believe that the present work on water-soluble resorcinarenes can greatly improve our understanding of the size/shape matching efficiency and molecular binding mechanism in this promising but less known area of calixarene and supramolecular chemistry.

RESULTS AND DISCUSSION

Synthesis and Characterization of SR4A5. The synthetic route for the modified calix[4]resorcinarene bearing sulfonate sites and *n*-pentyl chains (SR4A5) is described in Scheme 1.

Scheme 1. Synthesis of the Host SR4A5 and the Selected Quaternary Ammonium Guests G1−G9

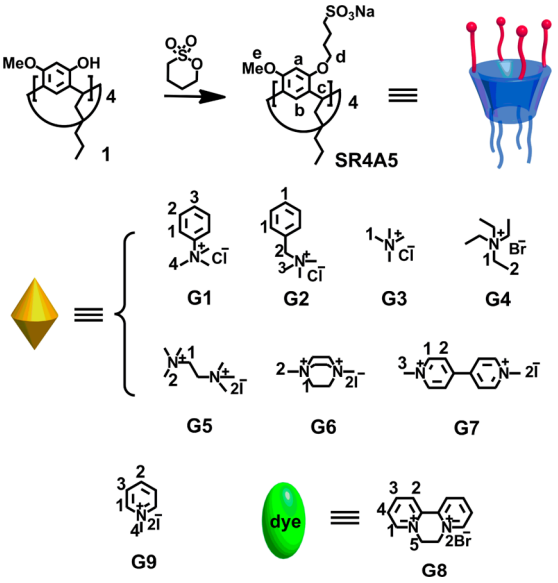

The precursor, tetramethoxyresorcinarene **1**, was prepared from 3-methoxyphenol and caproaldehyde by an improved procedure, and it was found that the constant reaction temperature was a crucial factor to obtain the target compound **1** in satisfactory yield (see the Experimental Section).[12] Then the water-soluble calix[4]resorcinarene host SR4A5 was obtained by the reaction of **1** with 1,4-butane sultone in 43% yield and comprehensively verified by NMR spectroscopy, high-resolution mass spectrometry, and elemental analysis (Figures S2−S4 and S43−S44 in the Supporting Information).[13]

Because it possesses hydrophilic sulfonate units at the upper rim of the resorcinarene and hydrophobic alkyl tails at the lower rim, the host compound SR4A5 was expected to display typical amphiphilic characteristics. Therefore, we preliminarily performed an electrical conductivity experiment to investigate the critical aggregation concentration (CAC) of host SR4A5. As illustrated in Figure S1 in the Supporting Information, the electrical conductivity gradually increased as the concentration of SR4A5 increased from 0.05 to 0.2 mM, accompanied by an inflection point at 0.3 mM, corresponding to the CAC value. When the concentration of SR4A5 is above the CAC, all of the added micelles are disassembled into monomers, and then the monomers are further diluted. Comparatively, when the concentration of SR4A5 is below the CAC, only the micellar solution can be diluted. Therefore, the UV/vis and steady-state fluorescence experiments in this work were accordingly performed below the CAC to avoid the undesirable micelle formation during the spectroscopic titrations. Moreover, no obvious change in peak pattern or chemical shift was observed above and below the CAC (Figure S5 in the Supporting Information), indicating that the proton signals in the NMR spectra cannot well reflect the aggregation state in SR4A5.

^{1}H NMR Titrations. According to the different types of substituents, the nine quaternary ammonium guests can be classified into four groups in our case: singly charged aliphatic ammonium salts (G3 and G4), doubly charged aliphatic ammonium salts (G5 and G6), singly charged π-aromatic ammonium salts (G1, G2, and G9), and doubly charged π-aromatic ammonium salts (G7 and G8). With these four kinds of guests in hand, we proceeded to analyze and discuss the influence of the guest structure, including the molecular size, shape, and charge number, on the binding stoichiometries and modes. ^{1}H NMR spectroscopic titrations were preliminarily performed to identify the binding geometries of resorcinarene with these guest molecules.[14] It is noteworthy that compared with the individual host, the peak pattern of the aromatic protons in SR4A5 (H_a and H_b) are dramatically split and broadened upon complexation with all of the guest molecules. These phenomena are mainly attributed to the cone shape of SR4A5 upon association, which can force the resorcinarene backbone to make closer contacts with guests. Moreover, the protons of the included guests underwent complex-induced upfield shifts to different degrees, mainly due to the strong shielding effect of the aromatic nuclei of the resorcinarene. For example, the aromatic protons of G8 exhibited a dramatic chemical shift change upon complexation with SR4A5 ($\Delta\delta_{H_2,G8\cdot SR4A5} = -1.16$ ppm and $\Delta\delta_{H_3,G8\cdot SR4A5} = -1.40$ ppm; Figure 1). Moreover, to explore the binding stoichiometries of the host−guest systems, Job plot experiments were performed, in which the molar ratio of SR4A5 and the guest was varied while the total molar concentration of the two components was kept constant. A typical Job plot for the complexation of G4

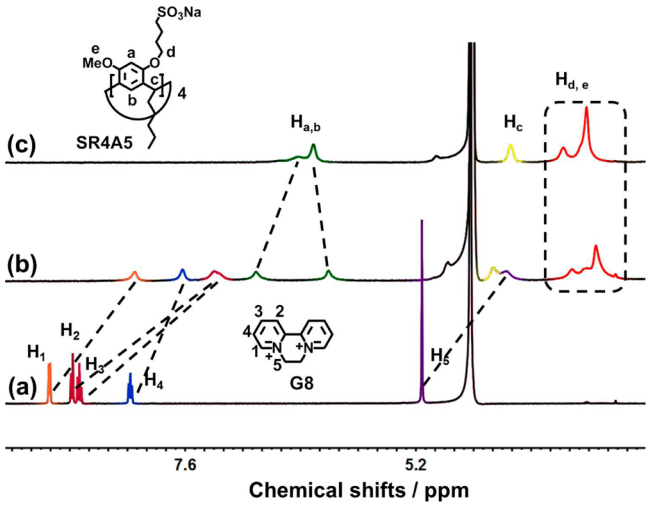

Figure 1. ^{1}H NMR spectra (400 MHz, D_2O, 25 °C) of (a) G8, (b) the G8·SR4A5 complex, and (c) SR4A5 ([G8] = [SR4A5] = 1 mM).

DOI: 10.1021/jo502825z
J. Org. Chem. 2015, 80, 1849−1855

with SR4A5 is shown in Figure 2. The plot of the chemical shift of H_1 on G4 versus the molar ratio gave an inflection point at

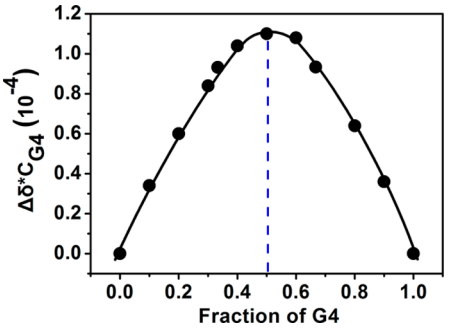

Figure 2. Job plot for G4 upon complexation with SR4A5 in D_2O ([G4] + [SR4A5] = 2.0 mM, 400 MHz, 25 °C).

0.5, revealing a 1:1 host−guest inclusion complex between SR4A5 and G4. Similar results were obtained in the association of SR4A5 with all of the examined guest molecules. It was also found that the complexation of SR4A5 with guests G1−G9 exhibits a fast-exchange equilibrium process, ultimately resulting in an averaged single resonance originating from both free and bound guest species on the ^{1}H NMR time scale. Meanwhile, quantitative analysis of the $\Delta\delta$ values, along with the cross-correlations in two-dimensional NMR spectroscopy experiments, provided abundant structural information about the spatial arrangements in the host−guest complexes.

Singly Charged Aliphatic Ammonium Salts (G3 and G4). ^{1}H NMR spectroscopy was employed to investigate the binding process of G3 and G4 with SR4A5. The $\Delta\delta$ values differed from each other, which could be used to deduce the binding geometries of the host−guest complexes because the proton with larger $\Delta\delta$ value would be more sensitive to the ring current effect of the aromatic nuclei in the resorcinarene. For guest G3, its methyl protons gave a slight upfield shift upon addition of an equimolar amount of SR4A5 ($\Delta\delta_{H_1,G3\cdot SR4A5}$ = −0.08 ppm; Figure S8 and Table S1 in the Supporting Information). Moreover, the chemical shift changes in G4·SR4A5 complex exhibited a similar tendency, indicating that the cavity of the resorcinarene can produce the same effect on the ethyl groups of G4 ($\Delta\delta_{H_1,G4\cdot SR4A5} \approx \Delta\delta_{H_2,G4\cdot SR4A5} \approx -0.14$ ppm, Figure S9 and Table S1 in the Supporting Information). Moreover, in the rotating-frame Overhauser effect spectroscopy (ROESY) experiments, the nuclear Overhauser enhancement (NOE) cross-peaks between the alkyl chains of SR4A5 and the ethyl groups of G4 definitely confirmed that the whole guest molecule was shallowly accommodated in the cavity from the upper rim of the resorcinarene (peaks A and B in Figure S16 in the Supporting Information).

Doubly Charged Aliphatic Ammonium Salts (G5 and G6). The complexation of SR4A5 with G5 and G6 was further investigated to identify the effect of charge on the host−guest binding process. Despite possessing two positive charges at the terminals, the aliphatic ammonium salts G5 and G6 maintained 1:1 binding stoichiometry with the host SR4A5, suggesting that the charge density of SR4A5 is negative enough to simultaneously accommodate the multiply charged substrates in its cavity (Figures S25−S28 in the Supporting Information). Moreover, the $\Delta\delta$ values for the G6·SR4A5 complex are slightly higher than the ones for the G5·SR4A5 complex, indicating that the spherical guest G6 may have a greater size-fit efficiency than the linear guest G5 toward the cone-shaped cavity of SR4A5 ($\Delta\delta_{H_1,G5\cdot SR4A5} \approx \Delta\delta_{H_2,G5\cdot SR4A5} \approx -0.18$ ppm and $\Delta\delta_{H_1,G6\cdot SR4A5} \approx \Delta\delta_{H_2,G6\cdot SR4A5} \approx -0.24$ ppm; Figures S10 and S11 and Table S1 in the Supporting Information). In addition, different from the singly charged salts, NOE correlations were observed between H_1 in G6 and the phenyl protons in the internal cavity of SR4A5 (Figure S17 in the Supporting Information), and this binding mode may be indicative of a higher intermolecular binding affinity in the G6·SR4A5 complex, which was further validated by the binding constants as described below.

Singly Charged π-Aromatic Ammonium Salts (G1, G2, and G9). To shed more light on the relationship between the binding mode and guest structural characteristics, we further investigated the complexation of SR4A5 with ammonium cations involving singly charged π-conjugation. Of these, guests G1 and G2 are comparable to G3 and G4 from the viewpoint of charge number and molecular size. However, by comparison of the $\Delta\delta$ sequences it was found that the binding geometries in the G1·SR4A5 and G2·SR4A5 complexes are quite different from those in the G3·SR4A5 and G4·SR4A5 complexes. As shown in Figure S6 in the Supporting Information, the $\Delta\delta$ values of G1 decreased in the order $H_3 > H_2 > H_1 > H_4$, and therefore, we can infer that G1 is immersed in the cavity of SR4A5 from the side of the phenyl ring to facilitate the intermolecular communication with the cavity, leaving the quaternary ammonium terminal of G1 surrounded by the alkylated sulfonate sites. An ^{1}H ROESY experiment was performed to obtain complementary information on the inclusion geometry of SR4A5 with G1. As discerned from Figures S14 and S15 in the Supporting Information, the G1·SR4A5 complex displays weak cross-peaks representing the correlations between H_1−H_3 of G1 and H_b at the upper-rim midsection of SR4A5 (peaks A and B). In addition, correlations between the positively charged terminal of H_4 in G1 and the hydrophobic alkyl chains of SR4A5 were observed (peaks C, D, and E), jointly confirming that G1 can penetrate into the cavity of SR4A5 along the longitudinal direction.

For guest G2, the $\Delta\delta$ values are in the order $H_1 \approx H_2 > H_3$ upon complexation with SR4A5. The protons H_1 in the phenyl ring and H_2 in the methylene group of G2 gave almost the same upfield shifts ($\Delta\delta_{H_1,G2\cdot SR4A5} \approx \Delta\delta_{H_2,G2\cdot SR4A5} \approx -0.34$ ppm; Figure S7 and Table S1 in the Supporting Information), indicating that these two sites are equally influenced by the host SR4A5. Therefore, it can be concluded that G2 can enter the cavity of SR4A5 along its latitudinal direction. Moreover, considering that there is no obvious cross-peak between G2 and the central phenyl ring of SR4A5 in ^{1}H ROESY spectrum, we can reasonablly infer that G2 is shallowly embedded in the upper rim of SR4A5 to satisfy the mutual electrostatic attraction between the positively charged quaternary ammonium groups and the negtively charged sulfonate sites. Compared with the rigidified molecule G1, the introduction of the benzyl group in G2 increases the molecular length and flexibility to some extent, making G2 more favorable to span the hydrophobic region at the upper rim with sulfonates and extended alkyl arms. However, SC4A can exclusively recognize the aliphatic sites of G1, whereas there is a rapid exchange between aromatic and aliphatic groups upon complexation of SC4A with G2 without specific regioselectivity.[15] The reported binding modes of SC4A with G1 and G2 are described in Figure S42 in the Supporting Information.

DOI: 10.1021/jo502825z
J. Org. Chem. 2015, 80, 1849−1855

Regarding the singly charged pyridinium G9, the $\Delta\delta$ values are arranged in the following sequence: $H_1 \approx H_3 > H_2 \approx H_4$ ($\Delta\delta_{H_1,G9\cdot SR4A5} \approx \Delta\delta_{H_3,G9\cdot SR4A5} \approx -0.9$ ppm; Figure S13 and Table S1 in the Supporting Information). Similar to the aforementioned G2·SR4A5 complex, the chemical shift changes in H_1/H_3 and H_2/H_4 here again demonstrate the longitudinal insertion of G9 into the cavity of SR4A5. In contrast to the G1·SR4A5 and G2·SR4A5 complexes, it is noted that the corresponding $\Delta\delta$ values of G9 are much larger than those of G1 and G2 upon complexation with SR4A5 under the same experimental conditions. Moreover, the NMR signals of the phenyl protons (H_a and H_b) are significantly split and broadended in the presence of G9, and meanwhile, the resonance of the methenyl groups (H_c) next to the phenyl rings of SR4A5 gave an obvious downfield shift upon complexation with G9 in water. These large disparities in the G9·SR4A5 complex demonstrate that G9 can penetrate into the cavity of SR4A5 more deeply, thus leading to the formation of a stable host–guest complex. Comparatively, it is known that G9 can enter the cavity of SC4A along the side of the phenyl ring with the positively charged $N-CH_3$ groups exposed to the sulfonate units, which is strikingly distinctive from the obtained G9·SR4A5 complex in our case.[9c] The deduced binding modes of G1, G2, and G9 with SR4A5 and SC4A are shown in Figure 3 and Figure S42 in the Supporting Information, respectively.

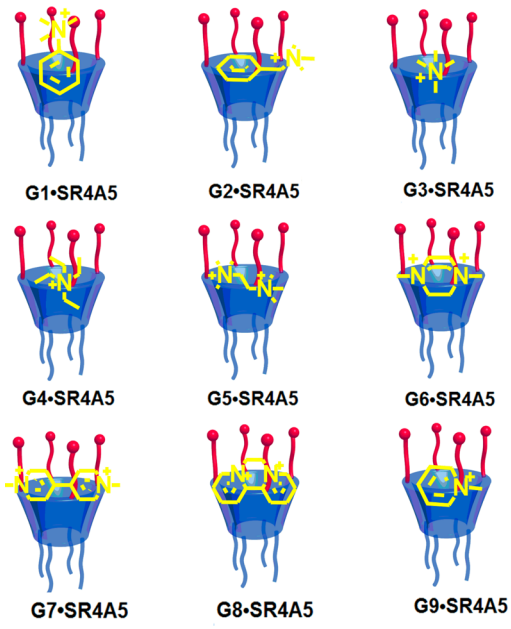

Figure 3. Possible binding modes of SR4A5 with guests G1–G9.

Through a careful comparison of the molecular structures of G1–G6 and G9, we can deduce that the host SR4A5 is always prone to entrap the organic cations with rigid and semirigid molecular structures, mainly through electrostatic attraction to the suspended sulfonate groups and inclusion complexation with the resorcinarene cavity. Thus, it was expected that SR4A5 may have a better binding affinity with the positively charged guests possessing larger π-aromatic cores.

Doubly Charged π-Aromatic Ammonium Salts (G7 and G8). Subsequently, guests G7 and G8 with doubly charged π-conjugation were further investigated by ^{1}H NMR spectroscopy. Studies of the binding behaviors of SR4A5 with G7 and G8 are beneficial to demonstrate the roles of π-conjugation and charge effects in the spatial arrangement of the host–guest complex (Figure 1 and Figure S12 in the Supporting Information). Moreover, it is noteworthy that the ^{1}H NMR signals of the aromatic groups in the G7·SR4A5 complex (H_1 and H_2) and the G8·SR4A5 complex (H_1–H_4) are remarkably broadened in the ranges of 7.21–7.74 and 7.24–8.14 ppm, respectively, in contrast to the sharp, high-resolution peaks for the complexes between SR4A5 and G1–G6. Furthermore, in comparison with the methyl protons next to the bispyridinium core ($\Delta\delta_{H_3,G7\cdot SR4A5} = -0.33$ ppm), the aromatic protons in G7 (H_1 and H_2) gave a dramatic upfield shift upon complexation with SR4A5 ($\Delta\delta_{H_1,G7\cdot SR4A5} \approx \Delta\delta_{H_2,G7\cdot SR4A5} \approx -1.09$ ppm), which is attributed to the effect of the ring current of the macrocyclic resorcinarene. Moreover, the corresponding $\Delta\delta$ values share similar characteristics in the G8·SR4A5 complex; that is, the aromatic protons situated at the bispyridinium center (H_2 and H_3) exhibit larger $\Delta\delta$ values (Figures 1), whereas the ones at the periphery of the positive charges (H_1, H_4, and H_5) display relatively smaller $\Delta\delta$ values. On the basis of these ^{1}H NMR titration results, it can be concluded that the complexes G7·SR4A5 and G8·SR4A5 adopt almost the same binding conformation, in which the bispyridinium moiety is deeply immersed into the cavity of SR4A5 along the longitudinal orientation while the positively charged terminals and nonaromatic groups are located at the upper rim of the resorcinarene (Figure 3). The possible binding mode of SR4A5 with G7 was further investigated by the molecular mechanics method to obtain the computed minimum-energy structure (Figure S45 in the Supporting Information). In contrast, there are essential differences in the SC4A-based complexes, in which the bispyridinium moieties in G7 and G8 are immersed into the cavity of SC4A with an acclivitous conformation[9c,d] (Figure S42 in the Supporting Information).

Fluorescence Spectroscopy. For the quantitative assessment of host–guest inclusion complexation, competitive binding titrations in water were performed by fluorescence spectroscopy. Through comparison of the UV/vis absorption spectra of host SR4A5 and guests G7–G9, it can be seen that G8 with relatively extensive π-conjugation has a unique absorption in the range from 300 to 350 nm (Figure S40 in the Supporting Information). Therefore, the excitation wavelength was set at 311 nm in the competitive binding titrations in order to avoid any light absorption from SR4A5 or other competitive guests. First, the photophysical behavior of the obtained G8·SR4A5 complex was examined by direct host–guest spectroscopic experiments, which showed significant fluorescence quenching of G8 upon gradual addition of SR4A5, probably due to the electronic communication between the electron-rich SR4A5 and the electron-deficient G8 (Figure S38 in the Supporting Information). According to the 1:1 binding stoichiometry in the G8·SR4A5 complex, the corresponding complex stability constant (K_S) was calculated to be 1.03×10^5 M^{-1} by a nonlinear least-squares curve-fitting method (inset of Figure S38 in the Supporting Information). Then, considering the appropriate binding affinity and good fluorescence responsiveness to SR4A5, G8 was chosen to serve as a spectral probe and competitive dye to investigate the inclusion complexation with other guest molecules. It was expected that the addition of excess amounts of guests could result in the disassembly of the G8·SR4A5 complex, as evidenced by the fluorescence recovery of unbound G8 (Scheme 2 and Figure 4).

DOI: 10.1021/jo502825z
J. Org. Chem. 2015, 80, 1849–1855

Scheme 2. Fluorescence "'Switch-On'" Displacement Assay for Analyte Sensing

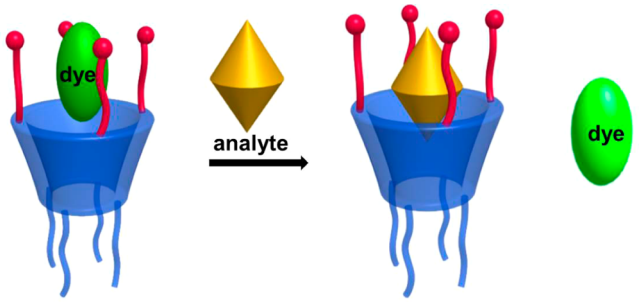

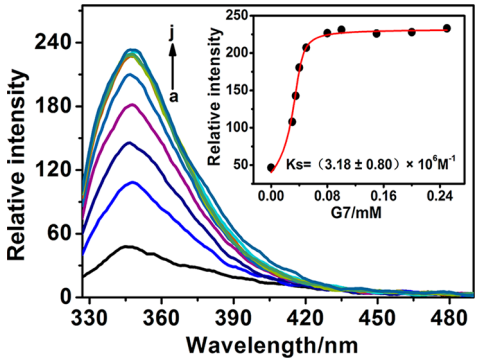

Figure 4. Competitive fluorescence titration of SR4A5 (40 μM) with G7 (0–0.25 mM from a to j) in the presence of G8 (5 μM) in water (pH 7.0, λ_{ex} = 311 nm, λ_{em} = 349 nm).

The fluorescence titration data could be used to obtain the corresponding K_S values by nonlinear fitting of the plots of the fluorescence intensity change (ΔF) against the total concentration of competitor guest (see Data Analysis and Fitting in the Supporting Information). For comparative purposes, K_S values for SC4A with the same guests in the reported literature are also listed in Table 1. In particular, the binding constant of G2 with SR4A5 was independently investigated by both direct and competitive titration methods to ensure the quantitative accuracy of the titration data. In the repeated measurements, the K_S values obtained from the different methods were reproducible within reasonable errors (Table 1).

Table 1. Complex Stability Constants (K_S/M^{-1}) for the Intermolecular Complexation of G1–G9 with SR4A5 and SC4A in Aqueous Solution (pH 7.0) at 25 °C

guest	K_S (SR4A5)	K_S(SC4A)	ref[a]
G1	(5.97 ± 1.38) × 10^2	4.0 × 10^4	9a
G2	(4.69 ± 1.16) × 10^2	1.3 × 10^4	9b
	(5.97 ± 1.13) × 10^2 [b]		
G3	(1.06 ± 0.19) × 10^2	7.9 × 10^4	9a
G4	(3.01 ± 0.42) × 10^2	4.0 × 10^3	9a
G5	(2.91 ± 0.37) × 10^3	–[c]	c
G6	(3.46 ± 0.24) × 10^3	(1.5 ± 0.1) × 10^7	9c
G7	(3.18 ± 0.80) × 10^6	(9.3 ± 0.1) × 10^5	9d
G8	(1.03 ± 0.14) × 10^5	(4.3 ± 0.1) × 10^7	9e
G9	(5.44 ± 0.55) × 10^2	(6.4 ± 0.3) × 10^5	9c

[a]The K_S values for SC4A-based complexes were obtained from ref 9. [b]This K_S value was obtained by direct host–guest titration. [c]This K_S value was not measured.

As discerned from Table 1, SR4A5 can form stable supramolecular complexes with all of the examined organic cations, with a maximum K_S of 3.18 × 10^6 M^{-1} for the G7·SR4A5 complex. It was also found that the K_S value is strongly affected by the charge number and π-conjugation. That is, the stability constants for the complexes with the doubly charged guests G5–G8 are obviously larger than those for the complexes with the singly charged guests G1–G4 and G9. Moreover, for the nonaromatic guests, the binding constant of SR4A5 with doubly charged G6 is 33 times higher than that with singly charged G3, whereas the binding constant is slightly (ca. 5 times) increased in complex G5·SR4A5 once the phenyl ring in G1 is replaced by the *N*,*N*,*N*-trimethylammonium group in G5. These results demonstrate that π-conjugation alone is not sufficient to form stable host–guest complexes with SR4A5 and that electrostatic attraction should be considered as the primary driving force governing the binding strength in the molecular recognition process. Therefore, upon coalescence of the superiority of both π-aromatic planes and multiple positive charges, it is not surprising that the complexation of SR4A5 with the electron-deficient guests G7 and G8 can be up to 10^7 M^{-1} order of magnitude in water, which overwhelms all of the thermodynamic stability in this work. Moreover, it is noted that although G9 possesses a structure similar to those of G7 and G8, the binding constants of SR4A5 with G7 and G8 seem not to be the simple sum of two individual compounds of G9, suggesting that there must be a strong interrelation between the preorganized electron-rich cavity of SR4A5 and the electron-deficient bispyridinium salts arising from their strict and favorable size-fit relationship to achieve the supramolecular cooperativity.

Furthermore, despite the fact that SC4A-based complexation always gives larger K_S values, the molecular selectivity is significantly improved in the case of SR4A5. It was found that the amphiphilic resorcinarene SR4A5 can readily distinguish the doubly charged π-aromatic substrates from other types of guest molecules. For example, the guest selectivity for aromatic G7 over nonaromatic G3 is as high as 3 × 10^4 ($K_{S,G7\cdot SR4A5}$/$K_{S,G3\cdot SR4A5}$ = 3 × 10^4), whereas this value is sharply decreased to only 12 in the complexation of SC4A with the same guests ($K_{S,G7\cdot SC4A}$/$K_{S,G3\cdot SC4A}$ = 12). This significant difference is ascribable to the molecular binding characteristics in SR4A and SC4A; that is, the former is prone to encapsulate the multiply charged π-aromatic substrates mainly through electrostatic attraction, whereas the latter can follow the rule of spherical shape complementarity between the guest and SC4A's conical cavity, which sometimes can override other known noncovalent forces, such as π-stacking and hydrophobic interactions.[16]

UV/Vis Spectroscopy. Apart from the regular electrostatic attraction to fix the relative orientations in SR4A5-involved binary complexes, we questioned whether the binding constants with guests G7 and G8 were noticeably increased by employing π-aromatic planes in the molecular recognition process. Inspired by the fluorescence quenching phenomena with G8 in the excited state, we continued to investigate the photophysical behaviors of G7·SR4A5 and G8·SR4A5 complexes in the ground state by means of UV/vis spectroscopy. It has been well-documented that face-centered stacking between electron-rich donors and electron-deficient acceptors can induce charge transfer (CT) absorbance in the long-wavelength region, which originates from π-orbital mixing through intermolecular nonbonded steric contacts.[17] As can be seen

DOI: 10.1021/jo502825z
J. Org. Chem. 2015, 80, 1849–1855

from Figure 5, a new absorption band was clearly observed in the range from 400 to 550 nm, corresponding to the CT

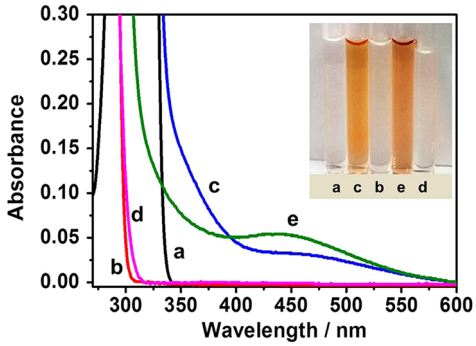

Figure 5. UV/vis absorption spectra and visible color changes of (a) G8, (b) SR4A5, (c) an equimolar mixture of G8 and SR4A5, (d) G7, and (e) an equimolar mixture of G7 and SR4A5 in water (pH 7.0) at 25 °C ([G7] = [G8] = [SR4A5] = 0.1 mM).

interaction in G7·SR4A5 and G8·SR4A5 complexes. Moreover, the molar absorption coefficient of the G7·SR4A5 complex ($\varepsilon_{G7\cdot SR4A5}$ = 5.4 × 10^2 L mol^{-1} cm^{-1}) is larger than that of the G8·SR4A5 complex ($\varepsilon_{G8\cdot SR4A5}$ = 3.4 × 10^2 L mol^{-1} cm^{-1}), indicative of a stronger donor−acceptor interaction between G7 and SR4A5. Consequently, the molecular binding affinity in the G7·SR4A5 complex is much greater than that in the G8·SR4A5 complex, which is well-consistent with the aforementioned fluorescence titration results ($K_{S,G7\cdot SR4A5}/K_{S,G8\cdot SR4A5}$ = 31; Table 1). Furthermore, in addition to the spectral changes, there is a visible color change upon complexation of SR4A5 with G7 and G8. That is, solutions of free SR4A5 and bispyridinium guest were colorless, but the mixed solution instantly turned yellowish-brown in the host−guest recognition process (Figure 5).

CONCLUSION

The amphiphilic calix[4]resorcinarene SR4A5 was newly synthesized, and its molecular binding behaviors with nine quaternary ammonium cations in water were systematically investigated. As shown by the spectroscopic observations, the bispyridinium guests G7 and G8 possessing multiple charge numbers and greater π-conjugation emerged into the limelight, benefiting from both the electrostatic attraction between the oppositely charged ionic components and the favorable CT interaction between the electron-rich resorcinarene cavity and the electron-deficient pyridinium centers. As a result, superior to the existing well-known SC4A systems, the SR4A5-involved binary complexation in this work reveals a much better molecular selectivity toward dicationic substrates, particularly toward bispyridinium derivatives. Moreover, the structure-dependent molecular binding behaviors further demonstrate that when supplemented by the appropriate charge distribution and molecular sizes, the effective utilization of CT interactions can offer a more powerful strategy to greatly facilitate the facile synergetic formation of stable supramolecular complexes. We also envision that the present study of bispyridinium−resorcinarene couples will not only deepen our understanding of positive supramolecular cooperativity in the specific molecular recognition process but also guide us in the fabrication of new resorcinarene-based supramolecular assemblies in water.

EXPERIMENTAL SECTION

Materials. The host SR4A5 was synthesized from 3-methoxyphenol and caproaldehyde in two steps. Guests G1−G4 were purchased from commercial sources and used without further purification. Guests G5−G9 were synthesized and purified according to the reported procedures.[7,18] The crystalline complexes were not obtained, probably because of the flexibility of the alkyl chains in SR4A5.

Measurements. NMR spectra were recorded on a 300 or 400 MHz spectrometer. The chemical shifts were recorded in parts per million. All of the chemical shifts were referenced to the internal acetone signal at 2.22 ppm. Coupling constant (J) values are shown in hertz. UV/vis and steady-state fluorescence spectra were recorded in a regular quartz cell (light path 1 cm) equipped with a temperature controller. The electrical conductivity in solution was measured using a conductivity meter at 25 °C. The geometry of the G7·SR4A5 complex was optimized by the molecular mechanics method with a Dreiding force field.

Preparation of Compound 1. A solution of 3-methoxyphenol (10 mL, 92.2 mmol) and caproaldehyde (11 mL, 92.2 mmol) in anhydrous CH_2Cl_2 (180 mL) was stirred under argon at 35 °C for 20 min. Then boron trifluoride diethyl etherate [$BF_3O(C_2H_5)_2$] (23 mL, 184.4 mmol) was added dropwise to the solution over 10 min. After the addition was complete, the reaction mixture was stirred for another 15 min and then washed with water and brine. The organic phase was dried and evaporated off. The obtained solid was recrystallized from methanol and water to yield **1** as a while solid. The characterization data are well-consistent with the reported results,[12] but the reaction time was greatly reduced from 2 h to 35 min. ^{1}H NMR (400 MHz, $CDCl_3$) δ 7.53 (s, 4H), 7.21 (s, 4H), 6.34 (s, 4H), 4.26 (t, J = 8.0 Hz, 4H), 3.82 (s, 12H), 2.18 (m, 8H), 1.32 (m, 24H), 0.89 (t, J = 6.8 Hz, 12H). HRMS (ESI) m/z [M + NH_4]$^+$ calcd for $C_{52}H_{72}O_8NH_4^+$ 842.5571, found 842.5571.

Preparation of Compound SR4A5. A solution of **1** (4.0 g, 4.8 mmol) and NaOH (0.84 g, 20.8 mmol) in THF (80 mL) and H_2O (20 mL) was stirred under argon at room temperature for 30 min. Then 1,4-butane sultone (2.1 mL, 20.4 mmol) was added to the solution. The resulting mixture was refluxed for 12 h and cooled. Then THF was removed by rotary evaporation under reduced pressure. The residue was dispersed into acetone and stirred for 30 min. The precipitate was filtered off and recrystallized from acetone and water to give SR4A5 as a pale-yellow solid in 43% yield (3.0 g). ^{1}H NMR (400 MHz, D_2O) δ 6.58 (s, 4H), 6.37 (s, 4H), 4.37 (s, 4H), 3.78 (s, 8H), 3.55 (s, 12H), 2.81 (s, 8H), 1.72 (s, 8H), 1.63 (s, 16H), 1.04 (s, 24H) 0.6 (s, 12H). ^{13}C NMR (100 MHz, D_2O) δ 155.4, 154.9, 126.5, 125.6, 98.4, 68.9, 55.9, 50.9, 35.1, 34.4, 32.0, 28.1, 27.1, 22.4, 21.1, 13.8. HRMS (ESI) m/z [M − 4Na + 3H]$^-$ calcd for $C_{68}H_{100}O_{20}S_4H_3^-$ 1367.5926, found 1367.5863. Anal. Calcd for $C_{68}H_{100}O_{20}S_4Na_4$: C, 56.03; H, 6.91; S, 8.80. Found: C, 56.05; H, 6.90; S, 8.81.

ASSOCIATED CONTENT

Supporting Information

Data analysis and fitting procedures, characterization data for compounds **1** and SR4A5, chemical shift changes upon host−guest complexation, 2D NMR spectra, Job plots, energy-minimized structures, and additional fluorescence and UV/vis spectroscopic titration results. This material is available free of charge via the Internet at http://pubs.acs.org.

AUTHOR INFORMATION

Corresponding Author

*E-mail: yuliu@nankai.edu.cn.

Notes

The authors declare no competing financial interest.

DOI: 10.1021/jo502825z
J. Org. Chem. 2015, 80, 1849−1855

■ ACKNOWLEDGMENTS

We thank the 973 Program (2011CB932502) and the National Natural Science Foundation of China (91227107 and 21102075) for financial support.

■ REFERENCES

(1) (a) Roberts, B. A.; Cave, G. W. V.; Raston, C. L.; Scott, J. L. *Green Chem.* **2001**, *3*, 280−284. (b) Tunstad, L. M.; Tucker, J. A.; Dalcanale, E.; Weiser, J.; Bryant, J. A.; Sherman, J. C.; Helgeson, R. C.; Knobler, C. B.; Cram, D. J. *J. Org. Chem.* **1989**, *54*, 1305−1312. (c) Egberink, R. J. M.; Cobben, P. L. H. M.; Verboom, W.; Harkema, S.; Reinhoudt, D. N. *J. Inclusion Phenom. Macrocycl. Chem.* **1992**, *12*, 151−158.

(2) (a) Guo, D.-S.; Uzunova, V. D.; Su, X.; Liu, Y.; Nau, W. M. *Chem. Sci.* **2011**, *2*, 1722−1734. (b) Shinkai, S.; Araki, K.; Matsuda, T.; Manabe, O. *Bull. Chem. Soc. Jpn.* **1989**, *62*, 3856−3862. (c) Koh, K. N.; Araki, K.; Ikeda, A.; Otsuka, H.; Shinkai, S. *J. Am. Chem. Soc.* **1996**, *118*, 755−758.

(3) Bombicz, P.; Gruber, T.; Fischer, C.; Weber, E.; Kálmán, A. *CrystEngComm* **2014**, *16*, 3646−3654.

(4) Zheng, D.-D.; Fu, D.-Y.; Wu, Y.; Sun, Y.-L.; Tan, L.-L.; Zhou, T.; Ma, S.-Q.; Zha, X.; Yang, Y.-W. *Chem. Commun.* **2014**, *50*, 3201−3203.

(5) (a) Bakirci, H.; Koner, A. L.; Dickman, M. H.; Kortz, U.; Nau, W. M. *Angew. Chem., Int. Ed.* **2006**, *45*, 7400−7404. (b) Bakirci, H.; Koner, A. L.; Schwarzlose, T.; Nau, W. M. *Chem.—Eur. J.* **2006**, *12*, 4799−4807. (c) Hennig, A.; Bakirci, H.; Nau, W. M. *Nat. Methods* **2007**, *4*, 629−632. (d) Nau, W. M.; Ghale, G.; Hennig, A.; Bakirci, H.; Bailey, D. M. *J. Am. Chem. Soc.* **2009**, *131*, 11558−11570. (e) Florea, M.; Nau, W. M. *Org. Biomol. Chem.* **2010**, *8*, 1033−1039. (f) Perret, F.; Lazar, A. N.; Coleman, A. W. *Chem. Commun.* **2006**, *23*, 2425−2438. (g) Perret, F.; Coleman, A. W. *Chem. Commun.* **2011**, *47*, 7303−7319.

(6) (a) Li, H.; Tan, L.-L.; Jia, P.; Li, Q.-L.; Sun, Y.-L.; Zhang, J.; Ning, Y.-Q.; Yu, J.; Yang, Y.-W. *Chem. Sci.* **2014**, *5*, 2804−2808. (b) Zhou, Y.; Tan, L.-L.; Li, Q.-L.; Qiu, X.-L.; Qi, A.-L.; Tao, Y.; Yang, Y.-W. *Chem.—Eur. J.* **2014**, *20*, 2998−3004. (c) Sun, Y.-L.; Zhou, Y.; Li, Q.-L.; Yang, Y.-W. *Chem. Commun.* **2013**, *49*, 9033−9035.

(7) Wang, K.; Guo, D.-S.; Zhang, H.-Q.; Zheng, X.-L.; Liu, Y. *J. Med. Chem.* **2009**, *52*, 6402−6412.

(8) (a) Javor, S.; Rebek, J., Jr. *J. Am. Chem. Soc.* **2011**, *133*, 17473−17478. (b) Amirov, R. R.; Mustafina, A. R.; Nugaeva, Z. T.; Fedorenko, S. V.; Kazakova, E. K.; Konovalov, A. I.; Habicher, W. D. *J. Inclusion Phenom. Macrocycl. Chem.* **2004**, *49*, 203−209.

(9) (a) Lehn, J.-M.; Meric, R.; Vigneron, J.-P.; Cesario, M.; Guilhem, J.; Pascard, C.; Asfari, Z.; Vicens, J. *Supramol. Chem.* **1995**, *5*, 97−103. (b) Arena, G.; Gentile, S.; Gulino, F.-G.; Sciotto, D.; Sgarlata, C. *Tetrahedron Lett.* **2004**, *45*, 7091−7094. (c) Zhao, H.-X.; Guo, D.-S.; Liu, Y. *J. Phys. Chem. B* **2013**, *117*, 1978−1987. (d) Qian, H.; Guo, D.-S.; Liu, Y. *Chem.—Eur. J.* **2012**, *18*, 5087−5095. (e) Hu, X.-Y.; Peng, S.; Guo, D.-S.; Ding, F.; Liu, Y. *Supramol. Chem.* **2014**, DOI: 10.1080/10610278.2014.967242.

(10) (a) Yoo, Y.-S.; Choi, J.-H.; Song, J.-H.; Oh, N.-K.; Zin, W.-C.; Park, S.; Chang, T.; Lee, M. *J. Am. Chem. Soc.* **2004**, *126*, 6294−6300. (b) Lee, M.; Jang, C.-J.; Ryu, J.-H. *J. Am. Chem. Soc.* **2004**, *126*, 8082−8083. (c) Discher, B. M.; Won, Y. Y.; Ege, D. S.; Lee, J. C. M.; Bates, F. S.; Discher, D. E.; Hammer, D. A. *Science* **1999**, *284*, 1143−1146. (d) Lee, M.; Lee, S.-J.; Jiang, L.-H. *J. Am. Chem. Soc.* **2004**, *126*, 12724−12725. (e) Sun, Y.; Yao, Y.; Yan, C.-G.; Han, Y.; Shen, M. *ACS Nano* **2010**, *4*, 2129−2142.

(11) (a) Zakharova, L. Y.; Syakaev, V. V.; Voronin, M. A.; Valeeva, F. V.; Ibragimova, A. R.; Ablakova, Y. R.; Kazakova, E. K.; Latypov, S. K.; Konovalov, A. I. *J. Phys. Chem. C* **2009**, *113*, 6182−6190. (b) Abis, L.; Dalcanale, E.; Vosel, A. D.; Spera, S. *J. Org. Chem.* **1988**, *53*, 5475−5479. (c) Högberg, A. G. S. *J. Am. Chem. Soc.* **1980**, *102*, 6046−6050.

(12) McIldowie, M. J.; Macerino, M.; Skelton, B. W.; White, A. H. *Org. Lett.* **2000**, *2*, 3869−3871.

(13) Shinkai, S.; Kawabata, H.; Arimura, T.; Matsuda, T. *J. Chem. Soc., Perkin Trans. 1* **1989**, 2039−2045.

(14) Fox, O. D.; Dalley, N. K.; Harrison, R. G. *J. Inclusion Phenom. Macrocycl. Chem.* **1999**, *33*, 403−414.

(15) Arena, G.; Casnati, A.; Contino, A.; Lombardo, G.-G.; Sciotto, D.; Ungaro, R. *Chem.—Eur. J.* **1999**, *5*, 738−744.

(16) Bakirci, H.; Koner, A. L.; Nau, W. M. *J. Org. Chem.* **2005**, *70*, 9960−9966.

(17) (a) Hunter, C. A.; Lawson, K. R.; Perkins, J.; Urch, C. J. *J. Chem. Soc., Perkin Trans. 2* **2001**, 651−669. (b) Martinez, C. R.; Iverson, B. L. *Chem. Sci.* **2012**, *3*, 2191−2201.

(18) (a) Gray, A. P.; O'Dell, T. B. *Nature* **1958**, *181*, 634−635. (b) Wempe, M. F. *J. Mol. Struct.* **2001**, *562*, 63−78. (c) Guo, D.-S.; Wang, L.-H.; Liu, Y. *J. Org. Chem.* **2007**, *72*, 7775−7778.

DOI: 10.1021/jo502825z
J. Org. Chem. 2015, 80, 1849−1855